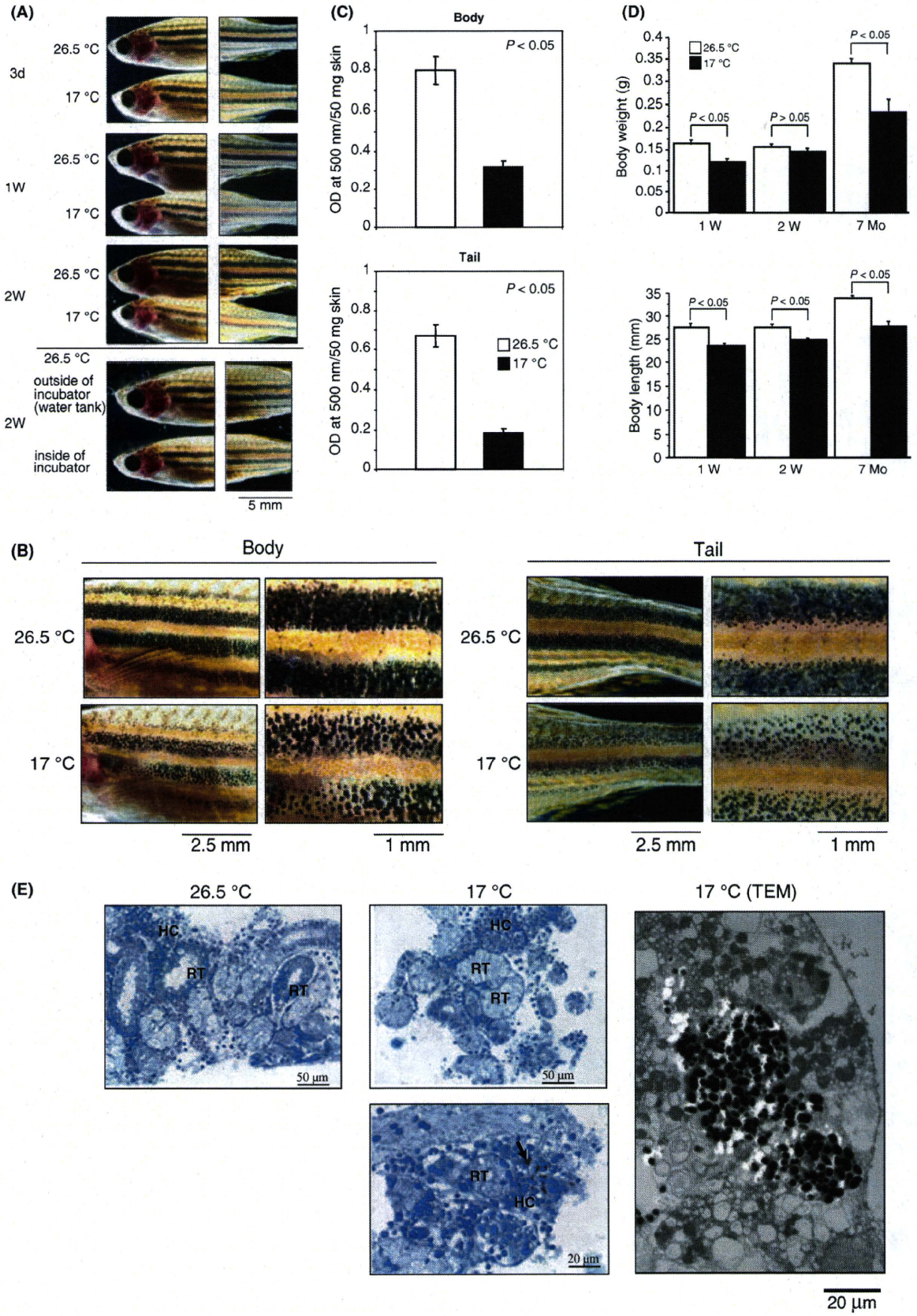

particularly tail, became paler than that of the normal zebrafish. After 2 weeks of cold exposure, the zebrafish pigmentation became even paler (Fig. 1A). High-magnification microscopy of the body flanks and tails showed that the melanophores of cold zebrafish appeared as small spots, as opposed to the larger spots of the normal zebrafish that covered wider area (Fig. 1B). We also assessed the changes in pigmentation before and after cold exposure in individual zebrafish. All cold zebrafish became paler than normal zebrafish (Fig. S1 in Supporting Information). To confirm the down-regulation of pigmentation in cold zebrafish, melanin content was measured by spectrophotometer. Melanin content in the body and tail skin of cold zebrafish was 2.7- and 3.5-fold lower than that of normal zebrafish (Fig. 1C). Moreover, to exclude the possibility that the color adaptation to white background occurred in cold zebrafish, we maintained zebrafish in 26.5 °C water inside of the incubator. The light cycle inside of incubator was controlled following the protocol of cold zebrafish maintenance. Two weeks later, the pigmentation of control zebrafish inside of incubator became slightly pale compared with that outside of incubator but was not severely down-regulated compared with cold zebrafish (Fig. 1A).

Cold exposure disrupts growth of zebrafish

The means and standard deviations of body weight and length were calculated from 6 to 7 zebrafish per group, and Student's *t*-test was used to determine statistical significance. There was a tendency that cold zebrafish had lower body weight and length than normal zebrafish at 1, 2 weeks and 7 months (Fig. 1D). Furthermore, abnormal renal tubules and melanophores were observed in the KM of cold zebrafish, but not in normal zebrafish (Fig. 1E, left and middle panels). To exclude the possibility that the abnormal melanophores were in fact melanin-containing macrophages, images of transmission electron microscopy (TEM) were captured. As shown in Fig. 1E (right panel) and Fig. S2 in Supporting Information, abnormal melanophores are not similar to macrophage in KM, implying that they were not melanin-containing macrophages.

Expression of *csdc2*, *hspa8* and *ef1a* genes in the skin of zebrafish

We next examined whether cold exposure altered the expression of genes encoding cold- and heat-shock proteins, such as *csdc2* and *hspa8*, and elongation factor 1a (*ef1a*), a constitutive gene (Tang *et al.* 2007). Zebrafish were sampled at day 3, 1 and 2 weeks of cold exposure. On day 3, expression levels of *csdc2* and *hspa8* genes in the skin of cold zebrafish were 2.2- and 1.5-fold higher than those of normal zebrafish, respectively (Fig. 2A). After 1 week of cold exposure, expression levels of *csdc2* in cold zebrafish slightly decreased, whereas expression levels of *hspa8* were threefold higher than those of normal zebrafish (Fig. 2A). After 2 weeks of cold exposure, expression levels of both *csdc2* and *hspa8* were not changed. Cold exposure did not alter the expression of *elfa* at all time points, suggesting that cold exposure mainly modulated the expression of *csdc2* and *hspa8*.

Up-regulation of *pmch* and down-regulation of *tyr* and *dct* in cold zebrafish

To understand further how cold exposure down-regulates the pigmentation of zebrafish, we investigated the expression levels of several genes known to be involved in pigmentation. In the brains of cold zebrafish, expression levels of *pomca*, which is involved in melanosome dispersion, were increased at week 1 and then decreased at week 2 (Fig. 2B). *Pmch*, which was involved in melanosome aggregation, remained unchanged at week 1, but increased at week 2 (Fig. 2B). Expression levels of *tyr* and *dct*, which are involved in melanin synthesis, were also investigated. *Tyr* expression was decreased at weeks 1 and 2 of cold exposure, whereas *dct* was decreased at week 1 and then recovered to normal levels at week 2 (Fig. 2B).

We then investigated the expression of genes involved in the differentiation of melanoblasts into melanocytes. *Mitfa*, *kita* and *kitlga* have been identified as indicators for melanocyte differentiation during fin regeneration (Rawls & Johnson 2000). Two weeks after cold exposure, expression levels of *mitfa* and *kita* in the skin of cold zebrafish were not significantly altered compared with normal zebrafish ($P > 0.05$), whereas that of *kitlga* was increased ($P < 0.05$) (Fig. 2C).

Cold exposure reduces the number of melanophores

Our results of morphological observation, melanin content and gene expression enabled us to suggest that the down-regulation of pigmentation in cold zebrafish was caused by (i) down-regulation of melanin synthesis and/or (ii) decrease in the number of melanophores. We then performed histological analyses of skin sam-

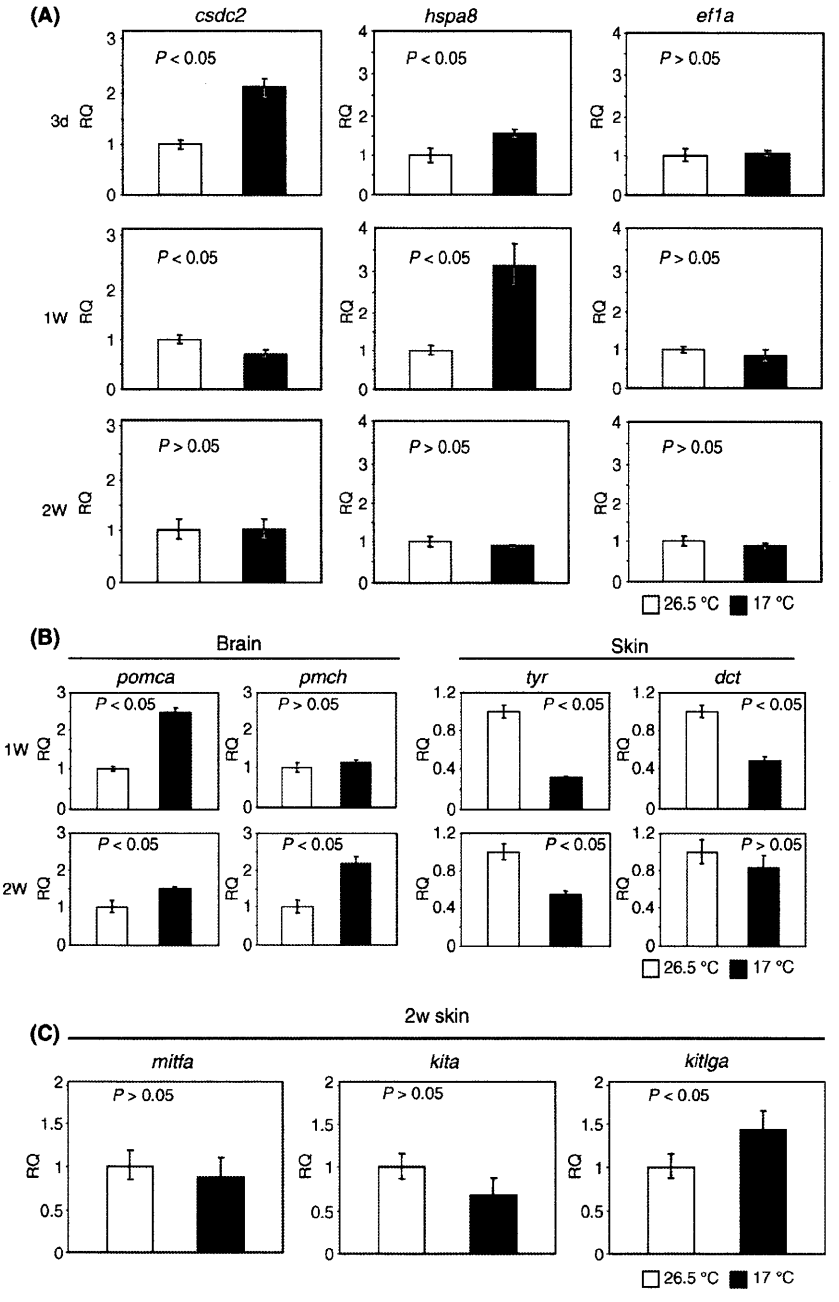

Figure 2 Expression levels of genes in normal and cold zebrafish (white and black bars, respectively). Levels of gene expression between normal and cold zebrafish were compared as relative quantities (RQ) on the *Y*-axis. (A) Expression levels of cold- and heat-shock protein genes, *csdc2* and *hspa8*, and a constitutively expressed gene, *ef1a*. Levels of *csdc2* and *hspa8* increased after 3 days (3 d) and 1 week (1 W) of cold exposure, whereas levels of *ef1a* were not changed. (B) Expression levels of genes involved in melanosome distribution, *pmoca* and *pmch*, and melanin synthesis, *tyr* and *dct*. In the brain of cold zebrafish, expression levels of *pmoca* increased at 1 W and slightly did at 2 W. Expression levels of *pmch* remained unchanged at 1 W, but increased at 2 W. In the skin, expression levels of *tyr* decreased both at 1 W and at 2 W, whereas *dct* decreased at 1 W and then recovered to normal levels. (C) Expression of genes involved in melanophore differentiation, *mitfa*, *kita* and *kitlga*, at the second week of cold exposure. Expression levels of *mitfa* and *kita* in cold zebrafish were not significantly different from normal zebrafish, whereas that of *kitlga* slightly was increased (~1.5-fold of normal zebrafish).

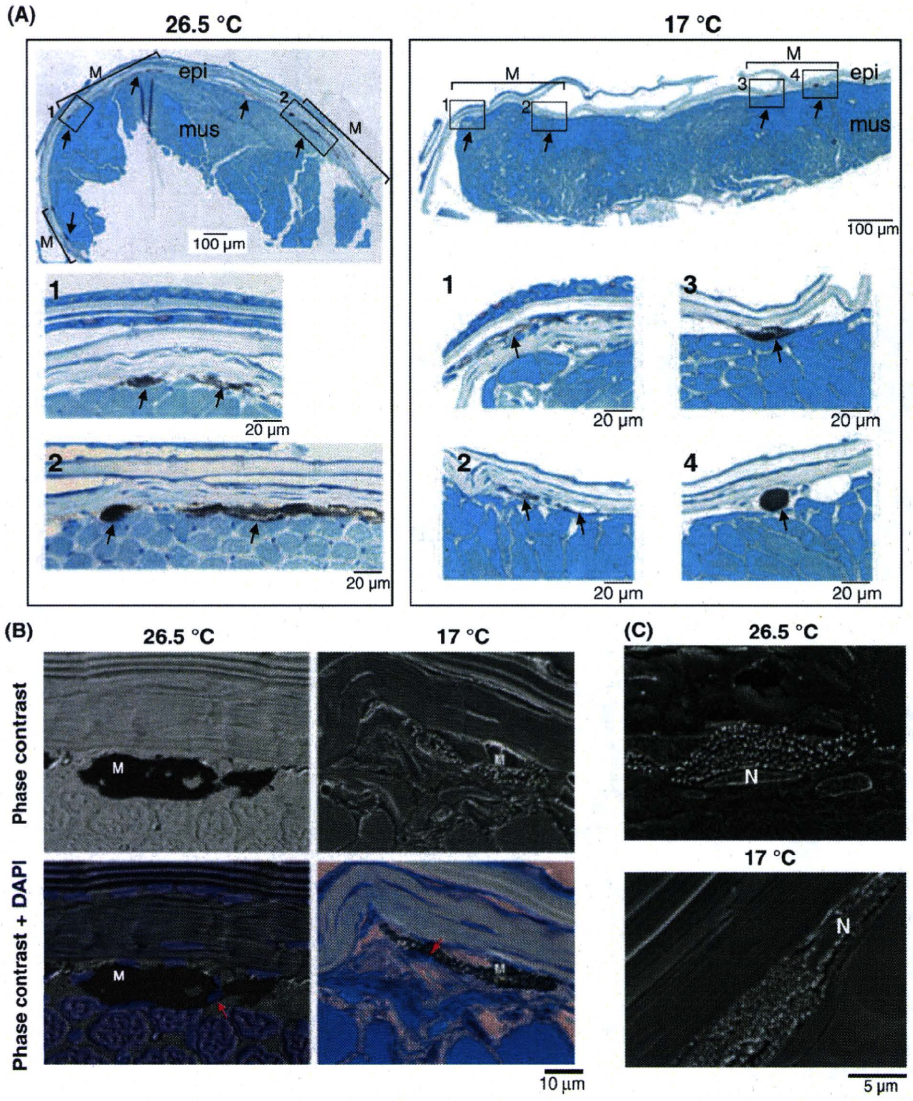

Figure 3 Histology of zebrafish skin. (A) Toluidine Blue O-stained zebrafish skin. Representative cross-sections of normal (26.5 °C) and cold (17 °C) zebrafish are shown. At lower magnification (upper panels), the number of melanophores (arrows) decreased in cold zebrafish. A series of melanophores (M) was localized between epidermis (epi) and muscle (mus) layers and named as melanophore band. The length of melanophore band in cold zebrafish (17 °C) was shorter than that of normal zebrafish (26.5 °C). At higher magnification (lower panels), the number of melanophores (arrows) decreased in melanophore bands of cold zebrafish compared with normal zebrafish. Lower panels are magnified view of boxes in upper panels. (B) Distribution of melanosomes in melanophores (M). Melanosomes were equally distributed in the cytoplasm of both normal and cold zebrafish. Nucleuses of melanophores were stained with DAPI and are located at the edge of cells (red arrows). There was no aggregation of melanosomes close to nucleus. (C) Images of scanning electron microscopy showed size, structure and distribution of melanosomes surrounding nucleus (N). There was no significant difference between normal and cold zebrafish.

ples using Toluidine Blue O staining and electron microscopy. At lower magnification (Fig. 3A, upper panels), we could observe a series of melanophores (arrows in upper panels of Fig. 3A) as if melanophores composed a band. The length of melanophore band in cold zebrafish (17 °C) was shorter than that of normal zebrafish (26.5 °C). When we examined a series of sections (results not shown), this observation was reproducible. At higher magnification, the number of melanophores decreased in the melanophore bands of cold zebrafish compared with normal zebrafish (Fig. 3A, lower panels). Taken together, it is likely that

the number of melanophores decreased in cold zebrafish. To investigate the distribution of melanosome in melanophores, we stained skin with DAPI that visualized nucleus. Melanosomes were equally distributed in the cytoplasm of both normal and cold zebrafish (Fig. 3B). There was no aggregation of melanosome close to nucleus (Red arrows in Fig. 3B). To quantify melanosome further, we performed scanning electron microscopy (SEM). Size and structure of melanosome in cold zebrafish were similar to normal zebrafish (Fig. 3C and Fig. S3 in Supporting Information). Taken together, cold exposure down-regulated adult zebrafish pigmentation through decreasing the number of pigmented melanophores.

Discussion

We have developed a novel model for pigmentation research. We show that adult zebrafish maintained at 17 °C water undergo depigmentation by decrease in pigmented melanophores. Overall melanin content in skin decreased without alteration in melanosome distribution in cold zebrafish. Pigment of adult zebrafish is composed of xanthophores, reflective iridophores and melanophores or melanocytes. Melanophore differentiation has been extensively studied during fin regeneration, and markers have been well described: *mitfa* for melanoblasts, *kita* for melanocytes and *tyr* and *dct* for pigmented melanophores (Rawls & Johnson 2000). In combination with these marker genes, we could evaluate melanophore differentiation and pigmentation. Expression levels of *mitfa* and *kita* genes remained unchanged, whereas that of *kitlga* was increased. It implies that melanophore differentiation was not altered and the increased expression of *kitlga* in cold zebrafish was because of a compensation mechanism. Although depigmentation in cold zebrafish was associated with *tyr* and *dct* down-regulation, decrease in the melanin-synthesizing enzymes does not certify the decrease in melanin because the activity of degradation enzyme might be down-regulated at low temperature. Gene expression of *try* and *dct* is identified in melanophores (Rawls & Johnson 2000; White & Zon 2008). The decrease in the number of melanophores might cause *tyr* and *dct* down-regulation in cold zebrafish.

Zebrafish have adaptation mechanisms that allow them to change the color of their pigment stripes within 24 h after background exposure (Logan *et al.* 2006); their pigmentation becomes lighter when exposed to white backgrounds and darker when exposed to black backgrounds. However, it is unlikely that the reduced pigmentation seen in cold zebrafish was because of background adaptation, because (i) we observed slight difference in pigmentation in zebrafish that were maintained inside or outside of the incubator and (ii) depigmentation occurred after 3 days of cold exposure, and not within 24 h (results not shown). This adaptation is caused by complex mechanisms existing in the endocrine and/or nervous systems (Fujii 2000). Melanosome aggregation in melanophores is also controlled by sympathetic neurons (Iwashita *et al.* 2006). Although gene expression of *pomca* and *pmch* encoding pro-hormones of melanocyte-stimulating hormone (MSC) and melanin-concentrating hormone (MCH), respectively, was up-regulated in cold zebrafish, there was no alteration in melanosome distribution in cold zebrafish, implying that sympathetic nervous system adjusted the melanosome distribution in cold zebrafish. It will be further necessary to investigate the involvement of nervous system in the future. Low temperatures down-regulate many physiologic processes (Sonna *et al.* 2002), but fish have compensatory mechanisms that allow adaptive survival in low temperatures (Cossins *et al.* 2002; Schwarzbaum *et al.* 1992a,b). In Arctic fish, it has been reported that the activity levels of ion pumps and Na^+/K^+-ATPases in the kidney are increased to balance the altered ion concentrations and body fluid pH caused by temperature acclimation (Schwarzbaum *et al.* 1992a,b). The abnormal renal tubules and melanophores in the KM of cold zebrafish might be due to similar adaptation mechanisms.

Cold- and heat-shock proteins are thought to play important roles in adaptation to cold exposure in vertebrates (Ali *et al.* 2003; Al-Fageeh & Smales 2006). Although their functions are not fully understood, it has been suggested that cold-shock proteins bind mRNA to regulate transcription and translation. We analyzed the expression levels of *csdc2* and *hspa8* genes in the skin of zebrafish to investigate the molecular relationships between cold exposure and pigmentation. Csdc2 contains an S1-like CSD, which is conserved in the cold-shock protein family proteins, and Hspa8 is one of the heat-shock protein 70 family proteins. It was reported that, under cold shock, Hspa8 is up-regulated in carp (Ali *et al.* 2003). In this study, gene expression of both *csdc2* and *hspa8* was up-regulated in the skin of cold zebrafish compared with normal zebrafish. This result implies that Csdc2 and Hspa8 directly or indirectly have a role in regulating pigmentation. Further investigation into this relationship is warranted.

In humans, abnormal melanin synthesis results in diseases such as hypopigmentation in albinism and hyperpigmentation in melasma, postinflammatory melanoderma and solar lentigines (Ni-Komatsu & Orlow 2007). Novel genes involved in the regulation of melanin synthesis can be potentially identified with this cold zebrafish model. Moreover, *dct* is associated with cisplatin-resistant malignant melanoma (Miller & Mihm 2006; Pak *et al.* 2004). However, the relationship between *dct* and melanoma biology still remains to be elucidated (White & Zon 2008). Further investigations to understand better the molecular mechanisms involved in the formation of malignant melanomas are warranted. Our cold zebrafish model may provide important insights into melanoma biology in the future.

Experimental procedures

Maintenance of zebrafish

Zebrafish (*Danio rerio*, India strain) born from the same parent were housed in tanks with recirculating dechlorinated tap water at 26.5 °C (room temperature) for 2 months. Two-month-old zebrafish were then separated into two groups: the first group was grown in 17 °C water inside an incubator for 3 days, 1, 2 weeks and 7 months and the second group was continuously maintained at 26.5 °C. Food, water and light cycles for both groups were controlled under the same conditions. To assess the presence of background adaptation in the incubators, one set of zebrafish was maintained inside and one set outside of the incubators in 26.5 °C water for 2 weeks, under the same conditions as mentioned earlier. The inside of incubator was covered by metal sheet.

Measurement of melanin content in zebrafish skin by spectrophotometer

Melanin content was measured following the method of Hultman & Johnson (2010) with a little modification. Zebrafish skin at body and tail was separately dissected out and weighted. Soluene®-350 (PerkinElmer, MA, USA) was added at a ratio 250 μL/50 mg skin and was heated at 95 °C for 1 h. After cooling, samples were centrifuged. Melanin in supernatant was assayed by absorption at 500 nm on a Nanodrop spectrophotometer (Thermo Fisher Scientific Inc.).

Growth measurement

Body weight and length were measured before killing the adult zebrafish to observe the effects of cold exposure on growth. Phenotypes were observed under a back-lit microscope (Olympus SZX16, Tokyo, Japan), and high-resolution

Table 1 Primer sets for zebrafish genes that are involved in pigmentation. Primers were designed using PRIMER EXPRESS® software version 3.0

Genes		Sequence (5′ → 3′)	Size (bp)	Reference sequences
bactin2	F	TGCTCCCCGAGCTGTCTT	64	NM_181601.3
	R	ACCAACCATGACACCCTGATG		
csdc2	F	CACACACCTCTCTCGCTTTCAT	100	NM_001002690.1
	R	TTGGCAGTGGACTCAGAGGTT		
dct	F	TTCACTCTCTGAGTCCGGAAGAG	100	NM_131555.1
	R	CAGTGCTGTGTGGCGATCAT		
ef1a	F	TCTACAAATGCGGTGGAATCG	100	NM_131263.1
	R	TCCAACACCCAGGCGTACTT		
hspa8	F	GATCGGCAGGAGGTTCGA	100	NM_001110403
	R	TTCCACTGCAACTTTTGGCTTT		
kita	F	ATCCTGCTCCACCTCAAATG	112	NM_131053.1
	R	GAGTAATGGGCTCCGTCAGA		
kitlga	F	GCCTGATGACCCCGAAAAA	100	XM_001922513.1
	R	CAAAACCACCACTGCGATTG		
mitfa	F	ATTCTTGGGTTCATGGATGCA	100	NM_130923.1
	R	CAGCTGGAGGAAGAGCATGAT		
pmch	F	TGGATGAGCAACGTAACGTAGAA	100	FJ392644.1
	R	TGCCAGCAGGGCCTGTATAC		
pomca	F	GAAGAGGAATCCGCCGAAA	98	NM_181438.3
	R	CCAGTGGGTTTAAAGGCATCTC		
tyr	F	GGTGCCCTTCATCCCTCTCT	100	NM_131013.1
	R	AAACCGCTGACCTGGATCCT		

TIFF images were acquired using an Olympus DP71 camera (Tokyo, Japan) attached to the microscope.

Dissection of zebrafish

Dissections were performed as previously described (Ivanovski *et al.* 2009). Briefly, adult zebrafish were anesthetized with 0.02% tricaine. Under the Olympus SZX16 (Tokyo, Japan), the superficial layers (outer epidermis and the underlying dermis) were carefully dissected out using two microforceps with 0.3-mm tips (World Precision Instruments, Sarasota, FL) and placed in RNA*later* (Life Technologies, Carlsbad, CA, USA). Muscles were dissected along the body. KMs, which are dark red-colored tissue with black dots and flanked by vertebral bones (Ivanovski *et al.* 2009), and brains were also dissected out and placed in RNA*later* (Life Technologies).

Real-time PCR

RNA extractions from skin, brain and KM were carried out using RiboPure™ kits (Life Technology), and mRNA was reverse-transcribed using High-Capacity RNA-to-cDNA kits (Life Technology). cDNA quality was evaluated by amplifying *bactin2*. Thirty thermal cycles were performed as follows: first denaturation at 95 °C for 10 s, annealing at 60 °C for 20 s and extension at 72 °C for 20 s. Gene expression levels were measured by StepOnePlus™ real-time PCR (Life Technology) using Fast SYBR® Green Master Mix. Primers were designed using PRIMER EXPRESS® software version 3.0 (Life Technology) and are shown in Table 1.

Histology of KM

Kidney marrows were fixed in 4% paraformaldehyde and 0.25% glutaraldehyde overnight. After three washes in PBS and once in 20% sucrose in PBS, the zebrafish were embedded into O.C.T. compound (SAKURA Tissue-Tek®; Torrance, CA, USA) and snap-frozen in liquid nitrogen before storage in −80 °C. For cryosections, the embedded zebrafish were cut cross-section into 10-μm slices and stained with Toluidine Blue O (Wako Pure Chemical Industries Ltd., Osaka, Japan). Stained cryosections were magnified at ×10, and the images were captured on an Olympus CKX41 microscope (Tokyo, Japan).

Histology of skin

Zebrafish were fixed in 0.1% paraformaldehyde and 4% glutaraldehyde overnight. After three washes in PBS, zebrafish were fixed in 2% OsO_4 at 4 °C for 2 h. Samples were dehydrated in 50%, 75%, 85% and 100% acetone for 10 min each. Dehydrated zebrafish were embedded in Technovit 8100 (Heraeus Kulzer GmbH, Hanau, German). The embedded zebrafish were cut cross-section into 3–4 μm by ultramicrotome (semi-thin) and stained with Toluidine Blue O (Wako Pure Chemical Industries Ltd.) or DAPI.

Electron microscopy

Scanning electron microscopy and TEM were performed as described by previously (Yahiro & Nagato 2005) with modification. For SEM, the embedded zebrafish were cut cross-section as semi-thin on Si-Chips. Ion etching was performed by hard mode 3 min × 2 times. Then, ion bombarder was performed by soft mode 3 min × 1 time. Tissues were coated with osmium (2.5 nm) and observed. For TEM, KMs were embedded in Epon 812 (Shell Chemical, San Francisco, CA, USA) and cut cross-section into 90 nm (ultrathin). Tissues were stained with uranyl acetate and lead and observed.

Acknowledgements

The authors acknowledge grant support from the Special Coordination Funds for Promoting Science and Technology and the Nagao Memorial Fund. Kasem Kulkeaw is a scholar of the Ajinomoto Scholarship Foundation, and Ognen Ivanovski is a research fellow of the Inoue Scientific Foundation. We also thank Drs. Sumio Isogai for many helpful discussions, and Dr Tomoko Inoue (Yokoo) and Mr Tatsuya Sasaki for their technical assistance.

References

Al-Fageeh, M.B. & Smales, C.M. (2006) Control and regulation of the cellular responses to cold shock: the responses in yeast and mammalian systems. *Biochem. J.* **397**, 247–259.

Ali, K.S., Dorgai, L., Abraham, M. & Hermesz, E. (2003) Tissue- and stressor-specific differential expression of two hsc70 genes in carp. *Biochem. Biophys. Res. Commun.* **307**, 503–509.

Cossins, A.R., Murray, P.A., Gracey, A.Y., Logue, J., Polley, S., Caddick, M., Brooks, S., Postle, T. & Maclean, N. (2002) The role of desaturases in cold-inducing lipid restructuring. *Biochem. Soc. Trans.* **30**, 1082–1086.

Fujii, R. (2000) The regulation of motile activity in fish chromatophores. *Pigment Cell Res.* **13**, 300–319.

Hultman, K.A. & Johnson, S.L. (2010) Differential contribution of direct-developing and stem cell-derived melanocytes to the zebrafish larval pigment pattern. *Dev. Biol.* **337**, 425–431.

Ivanovski, O., Kulkeaw, K., Nakagawa, M., Sasaki, T., Mizuochi, C., Horio, Y., Ishitani, T. & Sugiyama, D. (2009) Characterization of kidney marrow in zebrafish (*Danio rerio*) by using a new surgical technique. *Prilozi* **30**, 71–80.

Iwashita, M., Watanabe, M., Ishii, M., Chen, T., Johnson, S.L., Kurachi, Y., Okada, N. & Kondo, S. (2006) Pigment pattern in jaguar/obelix zebrafish is caused by a Kir7.1 mutation: implications for the regulation of melanosome movement. *PLoS Genet.* **24**, e197.

Johnson, S.L. & Weston, J.A. (1995) Temperature-sensitive mutations that cause stage specific defects in zebrafish fin regeneration. *Genetics* **141**, 1588–1595.

Kelsh, R.N. & Eisen, J.S. (2000) The zebrafish *colourless* gene regulates development of non-ectomesenchymal neural crest derivatives. *Development* **127**, 515–525.

Kulkeaw, K., Ishitani, T., Kanemaru, T., Fucharoen, S. & Sugiyama, D. (2010) Cold exposure down-regulates zebrafish hematopoiesis. *Biochem. Biophys. Res. Commun.* **394**, 859–864.

Lister, J.A., Robertson, C.P., Lepage, T., Johnson, S.L. & Raible, D.W. (1999) Nacre encodes a zebrafish microphthalmia-related protein that regulates neural-crest-derived pigment cell fate. *Development* **126**, 3757–3767.

Logan, D.W., Burn, S.F. & Jackson, J. (2006) Regulation of pigmentation in zebrafish melanophores. *Pigment Cell Res.* **19**, 206–213.

Malek, R.L., Sajadi, H., Abraham, J., Grundy, M.A. & Gerhard, G.S. (2004) The effects of temperature reduction on gene expression and oxidative stress in skeletal muscle from adult zebrafish. *Comp. Biochem. Physiol. C Toxicol. Pharmacol.* **138**, 363–373.

Miller, A.J. & Mihm, M.C. Jr (2006) Melanoma. *N. Engl. J. Med.* **355**, 51–65.

Ni-Komatsu, L. & Orlow, S.J. (2007) Identification of novel pigmentation modulators by chemical genetic screening. *J. Invest. Dermatol.* **127**, 1585–1592.

Pak, B.J., Lee, J., Thai, B.L., Fuchs, S.Y., Shaked, Y., Ronai, Z., Kerbel, R.S. & Ben-David, Y. (2004) Radiation resistance of human melanoma analysed by retroviral insertional mutagenesis reveals a possible role for dopachrome tautomerase. *Oncogene* **23**, 30–38.

Parichy, D.M., Ransom, D.G., Paw, B., Zon, L.I. & Johnson, S.L. (2000) An ortholog of the *kit*-related gene *fms* is required for development of neural crest-derived xanthophores and a subpopulation of adult melanocytes in the zebrafish *Danio rerio*. *Development* **127**, 3031–3044.

Parichy, D.M., Rawls, J.F., Pratt, S.J., Whitfield, T.T. & Johnson, S.L. (1999) Zebrafish sparse corresponds to an orthologue of c-kit and is required for the morphogenesis of a subpopulation of melanocytes, but is not essential for hematopoiesis or primordial germ cell development. *Development* **126**, 3425–3436.

Rawls, J.F. & Johnson, S.L. (2000) Zebrafish kit mutation reveals primary and secondary regulation of melanocyte development during fin stripe regeneration. *Development* **127**, 3715–3724.

Rawls, J.F. & Johnson, S.L. (2001) Requirements for the kit receptor tyrosine kinase during regeneration of zebrafish fin melanocytes. *Development* **128**, 1943–1949.

Schwarzbaum, P.J., Niederstätter, H. & Wieser, W. (1992a) Effects of temperature on the $(Na^+ + K^+)$-ATPase and oxygen consumption in hepatocytes of two species of freshwater fish, Roach (*Rutilus rutilus*) and Brook Trout (*Salvelinus fontinalis*). *Physiol. Zool.* **65**, 699–711.

Schwarzbaum, P.J., Wieser, W. & Cossins, A.R. (1992b) Species-specific responses of membranes and the $Na^+ + K^+$ pump to temperature change in the kidney of two species of freshwater fish, roach (*Rutulis rutulis*) and Arctic char (*Salvelinus alpinus*). *Physiol. Zool.* **65**, 17–34.

Sonna, L.A., Fujita, J., Gaffin, S.L. & Lilly, C.M. (2002) Invited review: effects of heat and cold stress on mammalian gene expression. *J. Appl. Physiol.* **92**, 1725–1742.

Tang, R., Dodd, A., Lai, D., McNabb, W.C. & Love, D.R. (2007) Validation of zebrafish (*Danio rerio*) reference genes for quantitative real-time RT-PCR normalization. *Acta Biochim. Biophys. Sin. (Shanghai)* **39**, 384–390.

White, R.M. & Zon, L.I. (2008) Melanocyte in development, regeneration, and cancer. *Cell Stem Cell* **3**, 242–252.

Yahiro, J. & Nagato, T. (2005) Application of ion etching to immunoscanning electron microscopy. *Microsc. Res. Tech.* **67**, 240–247.

Received: 26 July 2010
Accepted: 26 December 2010

Supporting Information/Supplementary material

The following Supporting Information can be found in the online version of the article:

Figure S1 Gross appearance of cold zebrafish before and after cold exposure.

Figure S2 Electron microscopic observation of zebrafish kidney marrow.

Figure S3 Electron microscopic observation of melanophore in skin of cold zebrafish.

Additional Supporting Information may be found in the online version of this article.

Please note: Wiley-Blackwell are not responsible for the content or functionality of any supporting materials supplied by the authors. Any queries (other than missing material) should be directed to the corresponding author for the article.

Stem Cell Rev and Rep (2011) 7:43–52
DOI 10.1007/s12015-010-9140-7

APOA-1 is a Novel Marker of Erythroid Cell Maturation from Hematopoietic Stem Cells in Mice and Humans

Tomoko Inoue · Daisuke Sugiyama · Ryo Kurita · Tatsuo Oikawa · Kasem Kulkeaw · Hirotaka Kawano · Yoshie Miura · Michiyo Okada · Youko Suehiro · Atsushi Takahashi · Tomotoshi Marumoto · Hiroyuki Inoue · Norio Komatsu · Kenzaburo Tani

Published online: 8 April 2010

Abstract The mechanism that regulates the terminal maturation of hematopoietic stem cells into erythroid cells is poorly understood. Therefore, identifying genes and surface markers that are restricted to specific stages of erythroid maturation will further our understanding of erythropoiesis. To identify genes expressed at discrete stages of erythroid development, we screened for genes that contributed to the proliferation and maturation of erythropoietin (EPO)-dependent UT-7/EPO cells. After transducing erythroid cells with a human fetal liver (FL)-derived lentiviral cDNA library and culturing the cells in the absence of EPO, we identified 17 candidate genes that supported erythroid colony formation. In addition, the mouse homologues of these candidate genes were identified and their expression was examined in E12.5 erythroid populations by qRT-PCR. The expression of candidate erythroid marker was also assessed at the protein level by immunohistochemistry and ELISA. Our study demonstrated that expression of the *Apoa-1* gene, an apolipoprotein family member, significantly increased as hematopoietic

Electronic supplementary material The online version of this article (doi:10.1007/s12015-010-9140-7) contains supplementary material, which is available to authorized users.

T. Inoue · R. Kurita · T. Oikawa · H. Kawano · Y. Miura · M. Okada · Y. Suehiro · A. Takahashi · T. Marumoto · H. Inoue · K. Tani (✉)
Department of Molecular Genetics,
Medical Institute of Bioregulation, Kyushu University,
3-1-1, Maidashi, Higashi-ku,
Fukuoka 812-8582, Japan
e-mail: taniken@bioreg.kyushu-u.ac.jp

T. Inoue
e-mail: yokotomo@bioreg.kyushu-u.ac.jp

R. Kurita
e-mail: k-ryo@brc.riken.jp

T. Oikawa
e-mail: oitatsullo@yahoo.co.jp

H. Kawano
e-mail: kawano@bioreg.kyushu-u.ac.jp

Y. Miura
e-mail: ymiura@bioreg.kyushu-u.ac.jp

M. Okada
e-mail: okadatch@bioreg.kyushu-u.ac.jp

Y. Suehiro
e-mail: suehiro@sentan.med.kyushu-u.ac.jp

A. Takahashi
e-mail: atsushi@sentan.med.kyushu-u.ac.jp

T. Marumoto
e-mail: marumoto@sentan.med.kyushu-u.ac.jp

H. Inoue
e-mail: hinoue@bioreg.kyushu-u.ac.jp

D. Sugiyama
Faculty of Medical Sciences, Department of Hematopoietic Stem Cells, SSP Stem Cell Unit, Kyushu University,
3-1-1, Maidashi, Higashi-ku,
Fukuoka 812-8582, Japan
e-mail: sugiyama@hsc.med.kyushu-u.ac.jp

K. Kulkeaw
Faculty of Medical Sciences, Department of Hematopoietic Stem Cells, SSP Stem Cell Unit, Kyushu University,
3-1-1, Maidashi, Higashi-ku,
Fukuoka 812-8582, Japan
e-mail: kkulkeaw@yahoo.com

N. Komatsu
Department of Transfusion Medicine and Stem Cell Regulation,
Juntendo University School of Medicine,
2-1-1, Hongo, Bunkyo-ku,
Tokyo 113-8431, Japan
e-mail: komatsun@juntendo.ac.jp

stem cells differentiated into mature erythroid cells in the mouse FL. The Apoa-1 protein was more abundant in mature erythroid cells than hematopoietic stem and progenitor cells in the mouse FL by ELISA. Moreover, *APOA-1* gene expression was detected in mature erythroid cells from human peripheral blood. We conclude that APOA-1 is a novel marker of the terminal erythroid maturation of hematopoietic stem cells in both mice and humans.

Keywords APOA-1 · Erythroid cell maturation · Fetal liver erythropoiesis · Library screening · Lentiviral cDNA library

Introduction

Hematopoiesis is the process in which pluripotent hematopoietic stem cells (HSCs) are generated, differentiated into specific progenitors, and ultimately matured into a variety of blood cell types (erythrocytes, megakaryocytes, lymphocytes, neutrophils, and macrophages) [1]. During embryonic development, HSCs emerge in the aorta-gonad-mesonephros (AGM) region and expand first in the fetal liver (FL) and then in the bone marrow (BM) [2–5]. Among these hematopoietic organs, the FL is a site of both HSC expansion and active erythropoiesis [6]. Erythropoiesis is the process by which a vast number of enucleated red blood cells (RBCs) are produced from hematopoietic stem cells (HSC) [7]. However, the molecular mechanisms underlying erythropoiesis have not been fully elucidated, largely because there are only a few molecular markers of terminal erythroid maturation in both mice and humans. To address this issue, we focused on the events that regulate the terminal erythropoiesis of HSCs to mature erythroid cells in order to identify novel markers of mature erythrocytes.

A previous study established a mouse embryonic (ES) cell-derived erythroid progenitor (MEDEP) cell line [8]. Although erythroblasts expressing the erythroid maturation marker Ter119 [9] (a protein that molecularly resembles glycophorin) can be generated from ES/iPS-derived MEDEP cells, most of these cells remained nucleated, indicating that they have failed to complete terminal maturation. Ter119 antigen is currently the only erythroid-specific marker in mice. However, Ter119 is expressed at many maturation stages, from erythroblasts to mature, circulating erythrocytes. Therefore, additional markers for mature erythrocytes are needed. Numerous attempts at generating vast quantities of enucleated erythrocytes have failed to efficiently give rise to fully functional erythrocytes in vitro. This may in part be due to the gaps in our understanding of the mechanisms that regulate erythropoiesis.

The cytokine erythropoietin (EPO) plays important roles in erythropoiesis by regulating erythroid cell differentiation, maturation, proliferation, and survival. Erythroid cells are highly dependent on EPO during early differentiation and maturation but lose this dependency and express lower levels of the erythropoietin receptor (EPOR) as they mature [10]. We hypothesized that EPO-independent signaling plays an important role in the terminal stages of erythropoiesis.

We previously established a system in which specific lentiviral gene transduction induced hematopoiesis from embryonic stem cells of a nonhuman primate common marmoset in the absence of bone marrow stromal cells [11]. In addition, we constructed a high-performance human fetal liver (FL)-derived cDNA lentiviral library as a tool to facilitate the discovery of novel genes that are involved in the expansion of HSCs, erythropoiesis and/or liver development [12]. During embryogenesis, the FL is the major site of hematopoiesis, particularly erythropoiesis. Therefore, the FL-derived cDNA lentiviral library that we constructed contains many genes that are involved in the differentiation and maturation of these lineages. The goal of this study was to identify novel genes that are involved in or expressed during EPO-independent terminal erythroid maturation. We identified APOA-1 as a novel marker of the maturation of hematopoietic stem cells into mature erythroid cells.

Materials and Methods

Cells

UT-7/EPO cells [13] (kindly provided by Dr. Komatsu) are an EPO-dependent cell line that was established from the bone marrow of a patient with acute megakaryoblastic leukemia. This cell line was cultured in Iscove's modified Dulbecco's medium (IMDM) supplemented with 10% fetal bovine serum (FBS) and 1 U/mL human recombinant EPO (R&D Systems, Minneapolis, MN) at 37°C in 5% CO_2.

Lentivirus Production

The previously generated human fetal liver-derived Entry cDNA library [12] was used in this study. Briefly, 34 μg ($1–2\times10^5$ cDNA clones) of the library was mixed with 20 μg of pCAG-HIVg/p and 20 μg of pCMV-VSVG-RSV-Rev as the packaging plasmids in 3.5 ml of FBS-free DMEM, and then 370 μl of 1 mg/ml polyethylenimine (PEI) was added to the mixture. After a 30-min incubation, the DNA/PEI complexes were dropped onto semi-

confluent 293 T cells in a T175 flask containing Opti-MEM medium and then incubated for 3 h. Next, these cells were cultured in DMEM containing 10% FBS. Virus-containing supernatants were harvested 4 days post transduction and concentrated by centrifugation (9,000 rpm, 6–8 h, 4°C). The virus pellet was resuspended in 1 ml of IMDM and used for overnight transduction of UT-7/EPO cells.

Transduction of the Lentiviral Library into UT-7/EPO Cells

UT-7/EPO cells were transduced with the viral cDNA library and cultured in methylcellulose semi-solid medium containing IMDM, 10% FBS, and P/S without EPO for one month. After this period, several colonies were harvested, and genomic DNA was isolated from each colony using the QIAamp DNA Micro Kit (Qiagen, Valencia, CA).

Genomic PCR and Sequence Analysis

The integrated cDNAs were PCR amplified using a forward primer (5′-TTCAGGTGTCGTGAACACGCTACCG-3′) and reverse primer (5′-CCTCGATGTTAACTCTAGAG GATCC-3′). The Expand Long Template PCR System (Roche, Basel, Switzerland) was used following the manufacturer's protocol. cDNAs that were cloned into the CSII-CMV-RfA vector were sequenced with the forward (5′-CAAGCCTCAGACAGTGG-3′) and reverse (5′-AGCG TATCCACATAGCG-3′) primers using a Big-Dye Terminator v3.1 Cycle sequencing kit (Applied Biosystems, Foster City, CA) and an ABI PRISM 3100 Genetic Analyzer (Applied Biosystems). The sequences were compared with the DNA database from the DNA Data Bank of Japan using BLAST.

Cell Culture and Sorting

The EPO-dependent UT-7/EPO cell line was established and cultured as previously reported [13]. C57BL6J mice and ICR mice were purchased from Nihon SLC. Twelve o'clock noon was considered to be 0.5 day postcoitum (dpc) for plugged mice. Fetal liver (FL) cells from a 12.5 dpc embryo were filtered through a 40 μM nylon mesh and washed with PBS. The cells were stained with a FITC-conjugated anti-mouse CD71 Ab (BD Biosciences), PE-conjugated anti-mouse Sca-1 Ab (BD Biosciences), APC-conjugated anti-mouse c-Kit Ab (BD Biosciences), PE-Cy7-conjugated anti-mouse CD45 Ab (eBioscience) and APC-Cy7-conjugated anti-mouse Ter119 Ab (eBioscience). The cells were sorted using a FACS Aria cell sorter (BDIS), and the data files were analyzed using FlowJo software (Tree Star, Inc.).

Human peripheral blood (PB) was obtained from healthy volunteers. The PB was stained with a FITC-conjugated anti-human CD45 Ab (eBioscience), PE-conjugated anti-GPA antibody (eBioscience) and APC-conjugated anti-human CD41 antibody (BD Bioscience). The cells were sorted using a FACS Aria cell sorter (BDIS), and the data files were analyzed using FlowJo software (Tree Star, Inc.).

All animal studies were approved by the Committee on Ethics in Animal Experiments of Kyushu University, and the human studies were approved by the Committee on Ethics in Human clinical samples of Kyushu University. All of these studies were performed following the guidelines of Kyushu University.

RNA Extraction and Real-time RT-PCR

Total RNA was isolated from FL cells of ICR embryos at 12.5 dpc or whole embryos at 10.5 dpc using the RNAqueous-4PCR kit (Ambion). Total RNA from human peripheral blood was isolated with the RiboPure Kit (Ambion). A high-capacity cDNA Archive kit (Applied Biosystems) was used to synthesize cDNA from RNA. The mRNA levels of various genes were analyzed by qRT-PCR using SYBR Green and gene-specific primers with the StepOnePlus real-time PCR system (Applied Biosystems). The mRNA level of each target gene was normalized to β-actin as an internal control.

Immunohistochemistry

Ter119-positive cells from 12.5 dpc FL cells were isolated by flow cytometry as described above. Cells were cytospun onto glass slides and air-dried. The cells were fixed in 1% PFA at room temperature (RT) for 10 min. Nonspecific binding was blocked by incubating the cells at RT for 30 min in a blocking solution containing 1% BSA and 0.05% Triton X-100 in PBS. The following antibodies were diluted in the blocking solution: rabbit anti-Apoa-1 (1:50, Santa Cruz Biotechnologies, Inc.). A donkey anti-rabbit IgG (H+L)-Alexa555 (1:250, Invitrogen) was used as secondary antibody and TOTO-3 (1:1500, Invitrogen) was added as a nuclear stain. Coverslips were mounted with fluorescent mounting medium (Dako), and the slides were examined using a confocal microscope (Olympus).

ELISA

c-Kit-positive cells and Ter119-positive cells were isolated by flow cytometry as described above. Proteins were extracted from the sorted cells using the Qproteome Mammalian Protein Preparation kit (Qiagen). To detect the Apoa-1 protein, a goat anti-Apoa-1 (0.8 μg/ml,

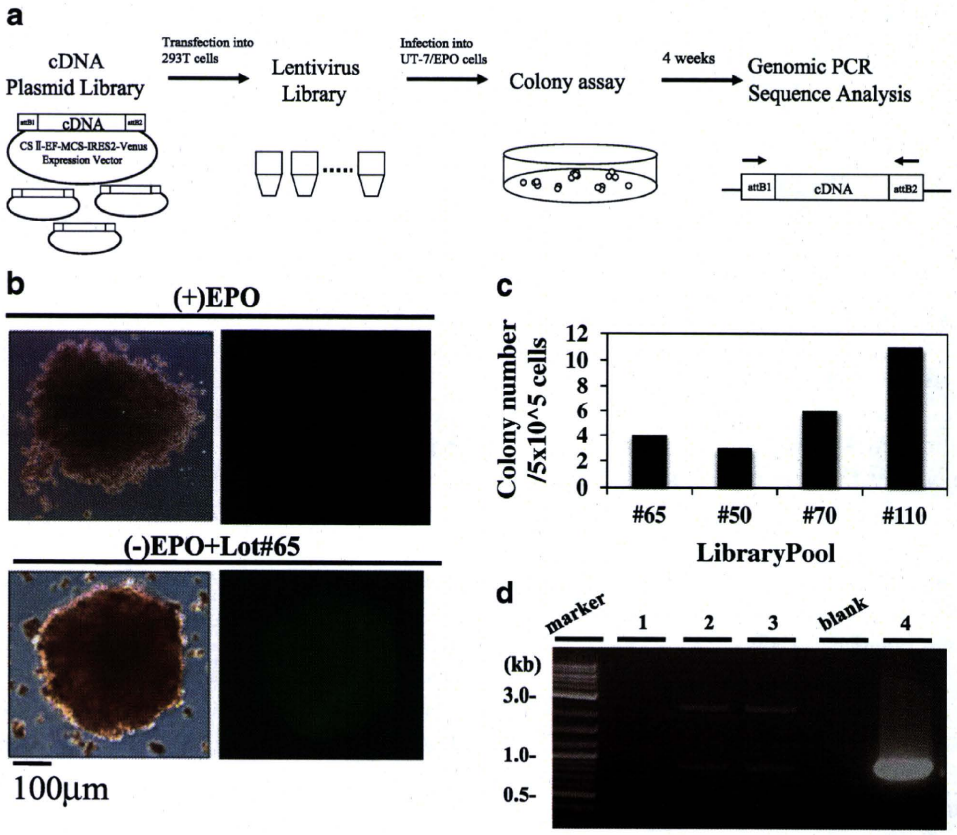

Fig. 1 Lentiviral human FL cDNA library screening in UT-7/EPO cells. **a** Strategy for identifying candidate EPO-independent regulators of erythropoiesis. Four pools (#65, #50, #70 and #110) of human FL-derived cDNA library were transfected into 293 T cells with helper plasmids to generate the lentiviral library. UT-7/EPO cells were transduced with these lentiviral library pools and then cultured in semisolid, EPO-deficient media for four weeks to positively select for clones that were able to form EPO-independent erythroid colonies. Finally, the cDNAs of the positive clones were sequenced to identify the transduced genes. **b** Erythroid colony assay. UT-7/EPO cells were transduced with the lentiviral pools (#65, #50, #70 and #110) and then transferred to semi-solid culture media. A representative colony derived from cells transduced with pool #65 is shown (Scale bar= 200 μm). A non-transduced colony was negative for Venus, while the lentiviral library-transduced colony was positive for Venus. **c** Colony number. A total of 22 colonies were obtained from UT-7/EPO cells that had been transduced with four lentiviral library pools and then analyzed by the colony formation assay. **d** Genomic PCR analysis. The inserted candidate genes were examined by genomic PCR using lentivirus insertion-specific primers. Lane 1: Untransduced UT-7/EPO cells (negative control), Lanes 2, 3: A colony derived from UT-7/EPO cells that had been transduced with lentiviral pool #65, Lane 4: GFP-transduced UT-7/EPO cells (positive control)

Rockland Immunochemicals) was used as a capture antibody, a rabbit anti-Apoa-1 (1:100, Santa Cruz Biotechnologies, Inc.,) was used as a detection antibody (primary antibody), and an anti-rabbit IgG-HRP (1:5000, Millipore) was used as the secondary antibody. Each antibody was captured onto 96-well immunoplates (Nunc) at 4°C for 16 h. Nonspecific binding was blocked by incubating the plate with 1% BSA/PBS for 2 h at RT. After the extracted proteins were added to the plate for 2 h at RT, the primary antibody was added for 1 h at RT, followed by the secondary antibody for 30 min at RT. The tetramethylbenzidine substrate was added to the wells for 30 min at RT, followed by a Stop Solution (R&D). The O.D. at 450 nm was measured using a Thermo Multiskan EX plate reader.

Results

Screening for Genes that Replace EPO/EPOR Signaling in UT-7/EPO Cells Using a Human FL Lentiviral Library

To identify novel genes that regulate erythroid cell maturation, we designed a strategy that monitored the ability of the EPO-dependent cell line, UT-7/EPO, to form erythropoietin (EPO)-independent colonies. Recently, we constructed a lentiviral human fetal liver (FL) cDNA library to search for novel genes that regulate hematopoiesis, including erythropoiesis [14]. Lentiviral cDNA library pools, which contained $1.32–1.98 \times 10^5$ cfu (colony forming units) per pool [14], were examined in this screen. We used the UT-7/EPO cell line, which is dependent upon EPO [13].

Table 1 Genes transduced in lentiviral-transduced erythroid colonies arising in the absence of Epo

Lentivirus pool #	Gene symbol	Discription
65	Angiotensinogen	AGT
	Estrogen receptor binding site associated antigen 9	EBAG9
50	B-cell CLL/lymphoma 2-like 1	BCL2-like 1
	Apolipoprotein A-1	APOA-1
70	ferritin heavy subunit	FHS
	3-phosphoinositide dependent protein kinase-1	PDPK1
	abl interactor 2	ABI-2
	Fibrinogen like 1	FGL1
	Apolipoprotein E	APOE
	Interferon induced transmembrane protein 2	1-8D
110	Asialoglycoprotein receptor 2	ASGR2
	Ferritin light chain	FLC
	Solute carrier family 27 (fatty acid transporter)	SLC27A2
	Ribosomal protein L10	RPL10
	Collagen type XVIII alpha 1	COL18A1
	Apolipoprotein J	APOJ
	Group-specific component	GC

When UT-7/EPO cells are transduced with genes in this lentiviral library that can functionally replace EPO/EPOR signaling, expression of these genes will result in colony formation in the absence of EPO (Fig. 1a). 293 T cells were transfected with four different lentiviral cDNA pools (#65, #50, #70 and #110). Subsequently, UT-7/EPO cells were transduced with these four different lentivirus library pools and cultured for four weeks in semi-solid media in the absence of EPO. Clones that acquired the ability to proliferate in the absence of EPO were identified and analyzed. Lentiviral-transduced cells were identified by Venus fluorescence that was encoded by the lentiviral vector. UT-7/EPO cells that were cultured in the absence of EPO failed to generate colonies, whereas these cells generated equal numbers of colonies when cultured in semi-solid media containing EPO (data not shown). When UT-7/EPO cells that had been transduced with the lentiviral library (6×10^5 cDNAs) were cultured in the absence of EPO, 22 EPO-independent colonies formed (Fig. 1b–c).

Next, to identify the cDNAs responsible for this EPO-independent proliferation, genomic DNA was isolated from each colony, and the integrated cDNAs were PCR amplified using lentivirus-specific primers (Fig. 1d). Agarose gel electrophoresis of the PCR products for each colony showed multiple bands of different sizes (Fig. 1d, lanes 2 and 3). This amplification was specific because untransduced UT-7/EPO cells did not yield any PCR products (lane 1), and a PCR product of the expected size was amplified from UT-7/EPO cells transduced with a lentivirus encoding green fluorescent protein (GFP) (lane 4).

Candidate Genes Identified from UT-7/EPO Cells Transduced with Human FL Lentiviral cDNA Library

The PCR products from the first round of screening were sequenced to identify the candidate genes that were expressed during erythropoiesis. Each pool contained a different number of inserted genes (Table 1). From the first screening, the following genes were identified as candidates that contributed to the growth of EPO-independent colonies; *FHS* and *FLC* encoding iron-binding proteins; the vitamin D-binding protein *GC*; the plasma protein receptor *ASGR2*; the vasoregulator *AGT*; estrogen-responsive protein *EBAG9*; the collagen *COL18A1*; the ribosomal protein *RPL10*; the kinase *PDPK1*; *ABI-2*, a kinase-binding protein; *APOA-1*, *APOE*, *APOJ* and *SLC27A2*, all of which encode lipid metabolism-related proteins; the anti-apoptotic protein *BCL2-like1*; and *1-8D*, encoding a protein of unknown function.

Among the integrated genes, some (*AGT*, *FHS*, *1-8D*, *FLC* and *GC*) were inserted into the host genome as a full-length coding sequence (CDS). As a result, these genes produced functional proteins that could be expressed in UT-7/EPO cells and lead to colony formation in the absence of EPO. Other genes (*BCL2-like1*, *APOA-1*, *PDPK1*, *FGL1*, *APOE*, *SLC27A2* and *COL18A1*) were inserted as a partial CDS that lacked the 5′ first start codons but contained 3′ stop codons, indicating that these genes were translated from a secondary start codon to the stop codon to yield partial proteins. As a result, functional proteins may be expressed in UT-7/EPO cells, leading to colony formation in the absence of EPO. The remaining inserted genes (*EBAG9*, *ABI-2*, *ASGR2* and *APOJ*) consisted of only a

Table 2 Gene specific primers for candidate genes in mice

Agt	5′	AGTGGGAGAGGTTCTCAATAGCA
	3′	GACGTGGTCGGCTGTTCCT
Ebag9	5′	GCAGCTACACAAGACATGCCTTT
	3′	TCCCACGCATTGCTATTTTCT
Bcl2-like1	5′	GGCTGGGACACTTTTGTGGAT
	3′	AAGCGCTCCTGGCCTTTC
Apoa-1	5′	GACAGCGGCAGAGACTATGTGT
	3′	AGGAGATTCAGGTTCAGCTGTTG
Fhs	5′	GCATGCCGAGAAACTGATGA
	3′	TCACGGTCTGGTTTCTTTATATCCT
Pdpk1	5′	TTCTTGGCGAGGGCTCTTT
	3′	CATATTCTCTGGAAGTGGCCAGTT
Abi-2	5′	GCGGGTGGCCGACTACT
	3′	TCTTCTAGGGCTCGCTGCTT
Apoe	5′	AGCTGCAGAGCTCCCAAGTC
	3′	TTACTTCCGTCATAGTGTCCTCCAT
1-8d	5′	CCTGGGCTTCGTTGCCTAT
	3′	CACATCGCCCACCATCTTC
Asgr2	5′	GGAGGAGAAGCAGCAACAGCTA
	3′	TGGGAAGTGCTTCAGGTGAAA
Flc	5′	CGGGCCTCCTACACCTACCT
	3′	GCCACGTCATCCCGATCA
Slc27a2	5′	CAACACACCGCAGAAACCAA
	3′	CCATTTCCCAGGGCTTTTTT
Rpl10	5′	TTCCATGTCATCCGTATCAACAA
	3′	CCCTGTCTGGAGCCTGTCA
Col18a1	5′	GCAGAGCCAGAGAATGTTGCT
	3′	CCCGACGTGAGGGTCATC
Apoj	5′	GGTCGGCCAGCAGCTAGAG
	3′	CGCCGTTCATCCAGAAGTAGA
Gc	5′	GGATCCTGCTGTACTTCTGCAA
	3′	TGCTTCATCTGGAGTCTCTCCTT

partial CDS without an open reading frame (ORF). These genes were translated from the shifted reading frame of the original mRNA and produced proteins of uncertain function. However, these genes resulted in UT-7/EPO colony formation in the absence of EPO. All of the 17 candidate cDNAs with full-length, partial or matched ORFs or partial but non-matched ORFs were examined in a secondary screen to identify specific genes that were involved in terminal erythroid maturation.

Expression of EPO-independent Growth-inducing Genes in Mouse FL Erythroid Populations

To determine which candidate genes obtained from first screen are critical for primary erythroid cell maturation, we performed a second screen to analyze gene expression during erythroid development. We used mouse fetuses for the second screen since mouse fetal samples are easier to obtain and use than human samples. The mouse homologues of these candidate genes were identified and the expression of the candidate genes was analyzed by RT-PCR using gene-specific primers (Table 2).

First, gene expression was assessed in samples from E10.5 whole embryos (WE) and E12.5 FL. All candidate genes were expressed in E12.5 FL with the exception of *Asgr-2,* which was eliminated as a gene of interest (Fig. 2). *Ebag9* and *Col18a1* expression was lower in the FL than in the whole E10.5 embryos, while *Fhs* and *Gc* had the opposite expression pattern with higher expression in the FL samples.

Next, we analyzed candidate gene expression in a series of FL-derived hematopoietic populations ranging from uncommitted hematopoietic stem cells (HSCs) to mature erythrocytes as determined by the expression of the surface markers CD45, Sca-1, c-Kit, CD71 and Ter119 (Fig. 3a). The following criteria were used to identify each hematopoietic population: (1) CD45+/Sca-1+/c-Kit+ cells represent HSCs; (2) c-Kit+ (Sca-1-/c-Kit+/CD71-/Ter119-) cells are BFU-E; (3) c-Kit+/CD71+ (Sca-1-/c-Kit+/CD71+/Ter119-) cells are committed erythroid progenitor cells or CFU-E; (4) CD71+/Ter119+ (Sca-1-/c-Kit-/CD71+/Ter119+) cells are proerythroblasts; and (5) Ter119+ (Sca-1-/c-Kit-/CD71-/Ter119+) cells represent mature erythroblasts and erythrocytes (Fig. 3a) [14, 15].

The mRNA expression of some candidate genes (*Abi-2*, *Slc27a2*) was higher in HSCs and gradually decreased throughout erythroid cell maturation (Fig. 3b). The expression of other candidate genes (*Pdpk1*, *Fhs*, *Flc*, *Rpl10*, *Ebag9* and *Apoe*) increased from HSCs to erythroblasts and then gradually decreased from erythroblasts to mature erythrocytes. *Bcl2l1* expression was low in HSCs and gradually increased. *Apoa-1* was highly expressed in

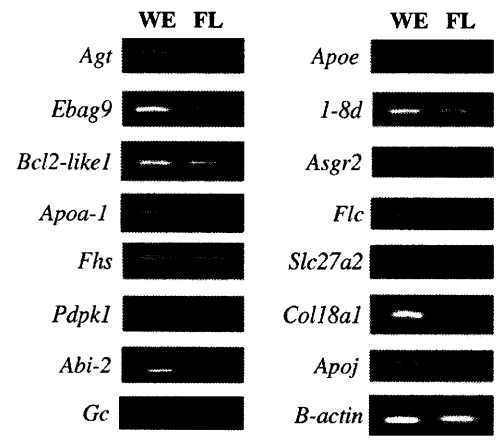

Fig. 2 Expression of candidate erythroid genes in developing mouse embryos. RT-PCR analyses of candidate genes in mouse embryos. We used RT-PCR to examine the expression patterns of the mouse homologues of each candidate gene in 10.5 dpc whole embryos (WE) and 12.5 dpc FL in ICR mouse embryos

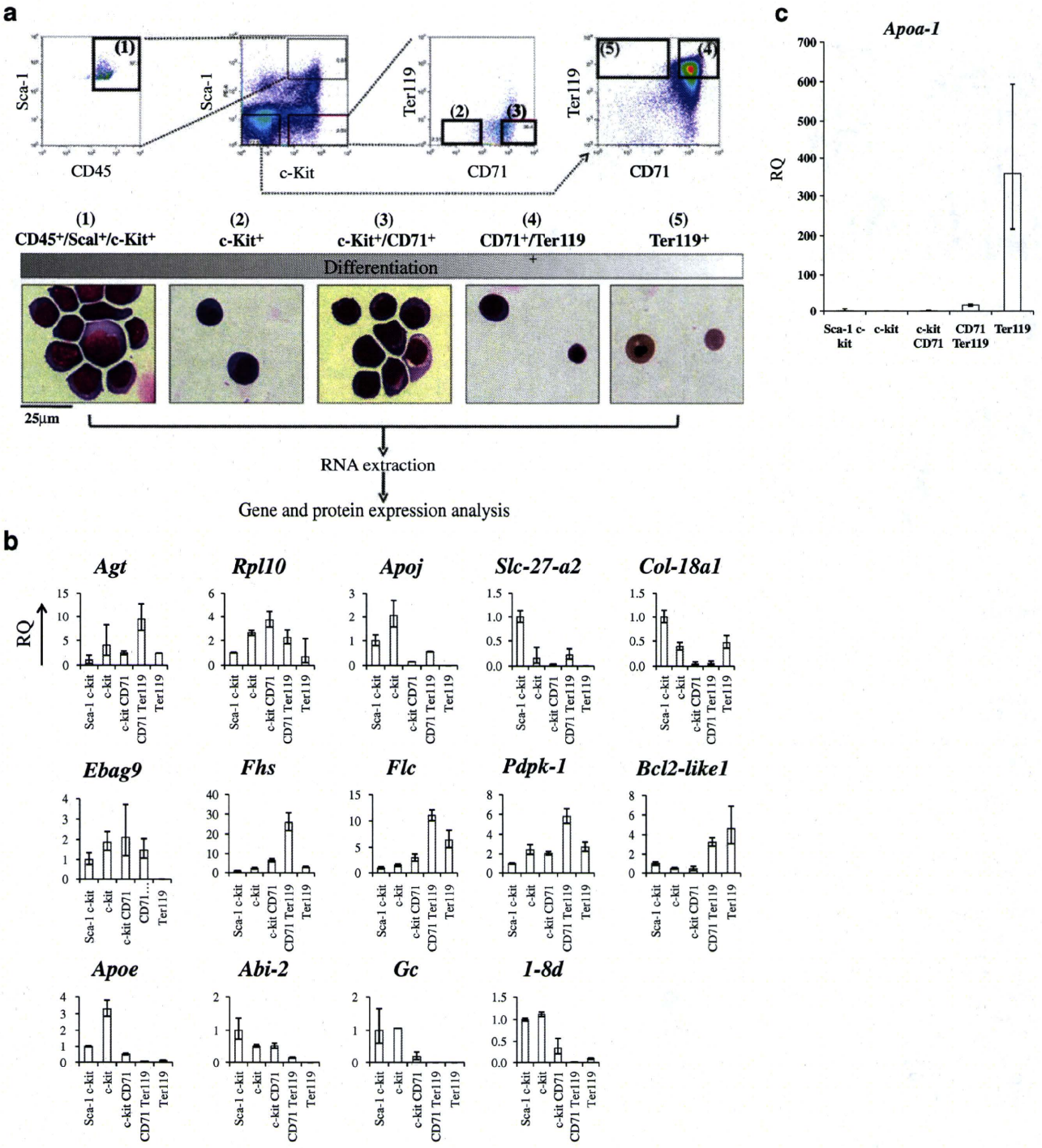

Fig. 3 Isolation of maturing erythroid populations from mouse FL cells. **a** Hematopoietic stem cells and maturing erythroid populations were isolated from 12.5 dpc mouse FL based on the expression of the surface markers CD45 (common leukocyte antigen), Sca-1 (stem cell antigen-1), c-Kit (stem cell factor receptor), CD71 (transferrin receptor) and Ter119 (Glycophorin A-associated antigen). The cytospins of each cellular fraction were prepared for May-Grunwald-Giemsa staining. As erythroid cells mature, the cell size decreased and finally the erythrocytes were enucleated. **b** mRNA expression patterns of candidate genes during erythroid cell maturation. The mRNA levels of candidate genes in maturing erythroid populations were analyzed by qRT-PCR. Total RNA was isolated from FL cells of 12.5 dpc embryos (Bars represent the means ± SD). The horizontal axes indicate the HSC fraction and the erythroid cell stage. Erythroid cell development proceeds from left to right. The vertical axes indicate the relative quantitation (RQ) of mRNA expression with the Sca-1$^+$/c-Kit$^+$ cell fraction set at an RQ value of 1. **c** The expression of mouse *Apoa-1* was significantly increased in the terminal maturation stages (Ter119$^+$ cell fraction) of cells obtained from 12.5 dpc FL

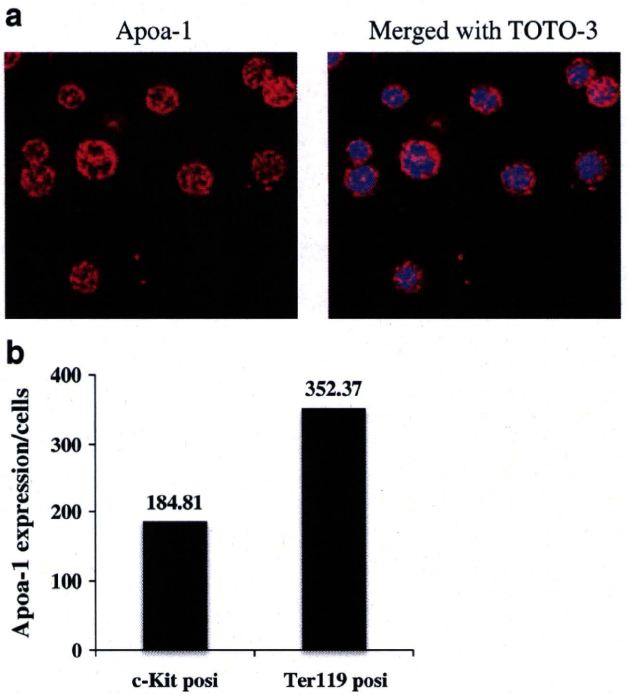

Fig. 4 Apoa-1 protein expression in mouse FL cells. **a** Immunohistochemistry. Ter119-positive cells from 12.5 dpc FL cells were cytospun and stained with an anti-mouse Apoa-1 antibody. Apoa-1-positive cells (*red*) were observed in 12.5 dpc FL cells. Nuclei were stained with TOTO3 (*blue*). **b** ELISA. c-Kit-positive cells and Ter119-positive cells from 12.5 dpc FL cells were sorted. Protein was extracted from each fraction and then analyzed by a sandwich ELISA. The expression levels of the mouse Apoa-1 proteins are shown for each fraction

Ter119-positive mature erythrocytes (Fig. 3c). The mRNA levels of *Apoa-1* increased approximately 350-fold, respectively, in the Ter119-positive cell population compared to the HSC population, suggesting that both of these genes are involved in the terminal maturation of erythroid cells.

Expression of the Apoa-1 Protein in Mouse FL Cells

To determine whether Apoa-1 is expressed at the protein level in mouse erythroid cells, immunohistochemical analyses were performed. Ter119-positive cells in mouse FL cells expressed the Apoa-1 protein (Fig. 4a). A sandwich enzyme-liked immunosorbent assay (ELISA) was also performed to quantitatively analyze the protein expression level in 12.5 dpc mouse FL cells. Because it is difficult to extract sufficient amounts of protein for an ELISA from individually fractionated cells in the populations shown in Fig. 3a, we compared the following two groups to analyze protein expression: c-Kit-positive cells, namely ((1)+(2)+(3) in Fig. 3) and Ter119-positive cells or ((4)+(5) in Fig. 3). As shown in Fig. 4b, Apoa-1 protein expression was approximately two-fold higher in Ter119-positive cells than c-Kit-positive cells, indicating that Apoa-1 expression correlates with terminal erythroid maturation at the protein level.

APOA-1 Expression in Human Peripheral Blood

To determine whether APOA-1 is useful as a terminal erythroid marker in human samples, we examined mRNA

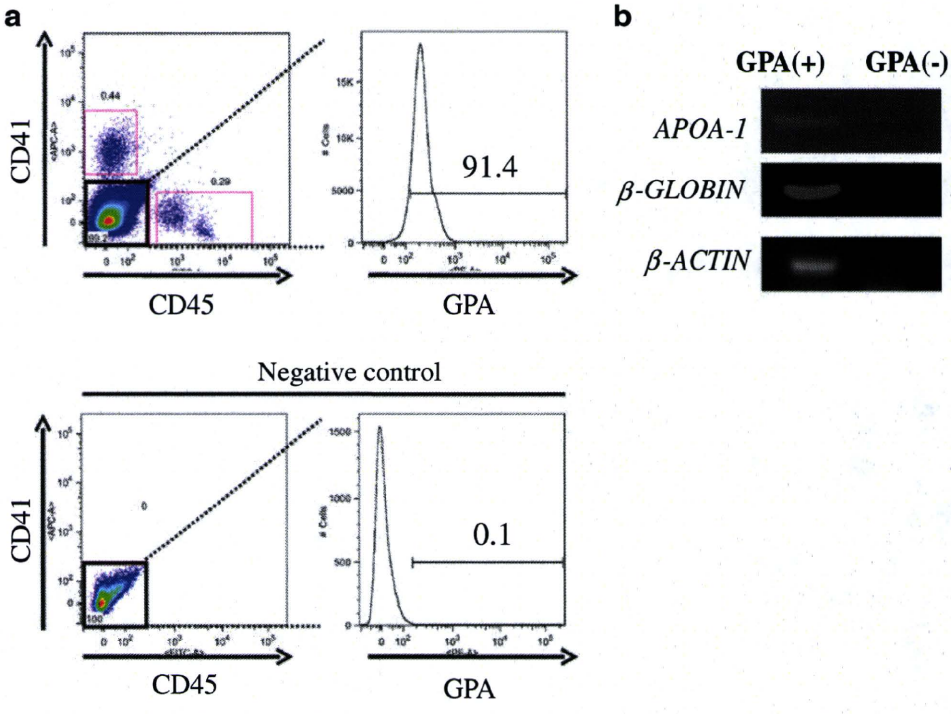

Fig. 5 *APOA-1* gene expression in human peripheral blood. **a** Erythrocytes and reticulocytes were isolated from human peripheral blood based on the expression of surface markers CD41 (integrin IIb), CD45 (common leukocyte antigen) and GPA (glycophorin A). **b** RT-PCR was performed to assess expression of human *APOA-1*. Human *β-GLOBIN* expression was analyzed to confirm that erythrocytes and reticulocytes had been isolated by flowcytometry. *APOA-1* was expressed in human peripheral blood

expression in human peripheral blood (PB) erythrocytes and reticulocytes. Erythrocytes and reticulocytes were isolated from peripheral blood by flow cytometry based on the expression of the cell surface markers glycophorin A (GPA), CD41 and CD45. In the PB, 91.4% of the CD41-/CD45-cells were positive for GPA (Fig. 5a). Reverse transcriptase PCR (RT-PCR) analysis showed that *β-GLOBIN* was expressed in GPA-positive cells, indicating that erythrocyte and reticulocyte mRNA was successfully extracted from the PB (Fig. 5b). Furthermore, *APOA-1* mRNA was expressed in the same fraction, demonstrating that this molecules can be used as a potential marker for terminal erythroid maturation in humans as well as mice.

Discussion

The goal of this study was to identify novel genes that are expressed during the terminal, EPO-independent maturation of erythroid cells. A two-step approach consisting of a lentiviral human FL cDNA library screen followed by an analysis of the gene expression patterns during erythropoiesis was performed to efficiently identify target genes.

This strategy had two clear advantages. First, it is important to establish a screening system that can detect erythropoiesis-related genes in an EPO-independent manner. A human FL cDNA library can be screened to identify novel genes. In this study, UT-7/EPO cells were transduced with a FL cDNA expression lentiviral library to detect genes that generate erythroid colonies in semi-solid medium in the absence of the EPO signaling pathway. Second, this screen could examine the effects of a large number (6×10^5) of genes on erythroid maturation. As humans are estimated to have approximately $2–3\times10^4$ genes, our screening encompassed a sufficient number of human cDNAs.

BCL2-like1 (BCL2L1) was one of the candidate genes identified in the first screen. *BCL2L1* encodes an anti-apoptotic protein that plays an important role in erythropoiesis in the absence of EPO [16]. Therefore, the results of our first screen strongly indicated that this system could be used to identify EPO-independent erythropoiesis-related genes. Other candidate genes included *FHS* and *FLC*, which encode iron-binding proteins, and *APOE, APOA-1, APOJ* and *SLC27A2,* which encode lipid metabolism-related proteins. Both iron and lipid metabolism are important cellular processes that regulate erythroid maturation [17–19]. We also identified a number of genes that were not previously implicated in erythropoiesis, including a vitamin D-binding protein (*GC*), vasoregulator (*AGT*), estrogen-responsive gene (*EBAG9*), collagen type 18 (*COL18A1*), ribosomal protein (*RPL10*) and several kinase-related proteins (*PDPK1* and *ABI-2*).

We also specifically identified a gene that was upregulated in the terminal stages of erythrocyte maturation. The identification of this gene is significant because very few molecular markers can be used to examine this stage of erythropoiesis. The candidate gene, *APOA-1*, was particularly interesting. APOA-1 is a major protein component of high-density lipoprotein (HDL) in the plasma and promotes the efflux of cholesterol from the tissues to the liver for excretion [20]. APOA-1 is a cofactor for lecithin cholesterol acyltransferase (LCAT), which is responsible for the formation of most plasma cholesteryl esters.

APOA-1 interacts with the ATP-binding cassette transporter ABCA1 (member 1 of human transporter sub-family ABCA) [21]. A recent report demonstrated that the APOA-1/ABCA1 pathway functions as an anti-inflammatory receptor by activating Janus Kinase 2 (JAK2)/Signal Transducers and Activation of Transcription3 (STAT3) in macrophages [22]. JAK2/STAT3 and/or JAK2/STAT5 are central signal pathways in erythroid cells [23]. Therefore, APOA-1/ABCA1 may activate the JAK2/STAT3 and/or JAK2/STAT5 pathway during the terminal maturation of erythroid cells.

It is intriguing to note that defects in APOA-1 are associated with low HDL levels observed in HDL deficiency type 1, which includes analphalipoproteinemia or Tangier disease. In Tangier disease patients, APOA-1 fails to associate with HDL. This inability to bind HDL is likely due to the faulty conversion of pro-APOA-1 molecules into mature chains, either due to a defect in the converting enzyme or a specific structural defect [24–26]. Furthermore, red blood cells in patients with Tangier disease have stomatocytosis and hemolytic anemia [27]. Moreover, patients with beta-thalassemia major as well as sickle cell disease have lower levels of APOA-1 in their plasma than healthy controls [28]. This abnormal erythrocyte morphology could be partially explained by a recent report by Holm TM et al., which showed that knockout mice with defects in the high-density lipoprotein receptor SR-BI have abnormal erythrocyte morphology. On the other hand, the fractional catabolic rate (FCR) for APOA-1 was significantly increased in patients with myeloproliferative disorders, including polycythemia vera, compared with healthy controls [29]. Therefore, accelerated red blood cell production could be also supported by increased APOA-1 catabolism. Further studies including both in vitro and/or in vivo analyses of APOA-1 knockouts are necessary to demonstrate the direct importance of APOA-1 in the maturation of red blood cells.

This study is the first to report that APOA-1 is a novel molecular marker for terminal erythroid maturation from HSC. In combination with Ter119 antigen or glycophorin A antigen, this molecule can potentially be used to identify mature erythrocytes in in vitro cultured erythroid cell

sources such as ES or iPS cells. It will be necessary to further investigate whether APOA-1 plays pivotal roles in erythroid cell maturation and is a useful maturation marker.

Acknowledgements The authors would like to thank Chiyo Mizuochi, Yuka Horio, Tatsuya Sasaki and Michiko Ushijima at Kyushu University for excellent technical assistance. This work was supported by a grant from the Project for Realization of Regenerative Medicine from the Ministry of Education, Culture, Sports, Science and Technology and by a grant from the BASIS project from the Ministry of Education, Culture, Sports, Science and Technology. T. Inoue is supported by research fellowships from the Japan Society for the Promotion of Science for Young Scientists.

Disclosures The authors indicate no potential conflicts of interest.

References

1. Weissman, I. L. (2000). Stem cells: units of development, units of regeneration, and units in evolution. *Cell, 100*, 157–168.
2. Mikkola, H. K., & Orkin, S. H. (2006). The journey of developing hematopoietic stem cells. *Development, 133*, 3733–3744.
3. Medvinsky, A., & Dzierzak, E. (1996). Definitive hematopoiesis is autonomously initiated by the AGM region. *Cell, 86*, 897–906.
4. Sugiyama, D., & Tsuji, K. (2006). Definitive hematopoiesis from endothelial cells in the mouse embryo; a simple guide. *Trends in Cardiovascular Medicine, 16*, 45–49.
5. Ema, H., & Nakauchi, H. (2000). Expansion of hematopoietic stem cells in the developing liver of a mouse embryo. *Blood, 95*, 2284–2288.
6. Palis, J. (2008). Ontogeny of erythropoiesis. *Current Opinion in Hematology, 15*, 155–161.
7. McGrath, K., & Palis, J. (2008). Ontogeny of erythropoiesis in the mammalian embryo. *Current Topics in Developmental Biology, 82*, 1–22.
8. Hiroyama, T., Miharada, K., Sudo, K., Danjo, I., Aoki, N., & Nakamura, Y. (2008). Establishment of mouse embryonic stem cell-derived erythroid progenitor cell lines able to produce functional red blood cells. *PLos One, 3*, e1544.
9. Kina, T., Ikuta, K., Takayama, E., et al. (2000). The monoclonal antibody TER-119 recognizes a molecule associated with glycophorin A and specifically marks the late stages of murine erythroid lineage. *British Journal Haematology, 109*, 280–287.
10. Zhang, J., Socolovsky, M., Gross, A. W., & Lodish, H. F. (2003). Role of Ras signaling in erythroid differentiation of mouse fetal liver cells: functional analysis by a flow cytometry-based novel culture system. *Blood, 102*, 3938–3946.
11. Kurita, R., Sasaki, E., Yokoo, T., et al. (2006). Tal1/Scl gene transduction using a lentiviral vector stimulates highly efficient hematopoietic cell differentiation from common marmoset (Callithrix jacchus) embryonic stem cells. *Stem Cells, 24*, 2014–2022.
12. Kurita, R., Oikawa, T., Okada, M., et al. (2008). Construction of a high-performance human fetal liver-derived lentiviral cDNA library. *Molecular and Cellular Biochemistry, 319*, 181–187.
13. Komatsu, N., Yamamoto, M., Fujita, H., et al. (1993). Establishment and characterization of an erythropoietin-dependent subline, UT-7/Epo, derived from human leukemia cell line, UT-7. *Blood, 82*, 456–464.
14. Suzuki, N., Suwabe, N., Ohneda, O., et al. (2003). Identification and characterization of 2 types of erythroid progenitors that express GATA-1 at distinct levels. *Blood, 102*, 3575–3583.
15. Walkley, C. R., & Orkin, S. H. (2006). Rb is dispensable for self-renewal and multilineage differentiation of adult hematopoietic stem cells. *Proceedings of the National Academy of Sciences of the United States of America, 103*, 9057–9062.
16. Dolznig, H., Habermann, B., Stangl, K., et al. (2002). Apoptosis protection by the Epo target Bcl-X(L) allows factor-independent differentiation of primary erythroblasts. *Current Biology, 12*, 1076–1085.
17. Gelvan, D., Fibach, E., Meyron-Holtz, E. G., & Konijn, A. M. (1996). Ferritin uptake by human erythroid precursors is a regulated iron uptake pathway. *Blood, 88*, 3200–3207.
18. Meyron-Holtz, E. G., Vaisman, B., Cabantchik, Z. I., et al. (1999). Regulation of intracellular iron metabolism in human erythroid precursors by internalized extracellular ferritin. *Blood, 94*, 3205–3211.
19. Holm, T. M., Braun, A., Trigatti, B. L., et al. (2002). Failure of red blood cell maturation in mice with defects in the high-density lipoprotein receptor SR-BI. *Blood, 99*, 1817–1824.
20. Breslow, J. L., Ross, D., McPherson, J., et al. (1982). Isolation and characterization of cDNA clones for human apolipoprotein A-I. *Proceedings of the National Academy of Sciences of the United States of America, 79*, 6861–6865.
21. Fitzgerald, M. L., Morris, A. L., Rhee, J. S., Andersson, L. P., Mendez, A. J., & Freeman, M. W. (2002). Naturally occurring mutations in the largest extracellular loops of ABCA1 can disrupt its direct interaction with apolipoprotein A-I. *Journal of Biological Chemistry, 277*, 33178–33187.
22. Tang, C., Liu, Y., Kessler, P. S., Vaughan, A. M., & Oram, J. F. (2009). The macrophage cholesterol exporter ABCA1 functions as an anti-inflammatory receptor. *Journal of Biological Chemistry, 47*, 32336–32343.
23. Richmond, T. D., Chohan, M., & Barber, D. L. (2005). Turning cells red: signal transduction mediated by erythropoietin. *Trends in Cell Biology, 15*, 146–155.
24. Zannis, V. I., Lees, A. M., Lees, R. S., & Breslow, J. L. (1982). Abnormal apoprotein A-I isoprotein composition in patients with Tangier disease. *Journal of Biological Chemistry, 257*, 4978–4986.
25. Gordon, J. I., Sims, H. F., Lentz, S. R., Edelstein, C., Scanu, A. M., & Strauss, A. W. (1983). Proteolytic processing of human preproapolipoprotein A-I. A proposed defect in the conversion of pro A-I to A-I in Tangier's disease. *Journal of Biological Chemistry, 258*, 4037–4044.
26. Schmitz, G., Assmann, G., Rall, S. C., Jr., & Mahley, R. W. (1983). Tangier disease: defective recombination of a specific Tangier apolipoprotein A-I isoform (pro-apo A-i) with high density lipoproteins. *Proceedings of the National Academy of Sciences of the United States of America, 80*, 6081–6085.
27. Reinhart, W. H., Gossi, U., Butikofer, P., et al. (1989). Haemolytic anaemia in analpha-lipoproteinaemia (Tangier disease): morphological, biochemical, and biophysical properties of the red blood cell. *British Journal Haematology, 72*, 272–277.
28. Sasaki, J., Waterman, M. R., & Cottam, G. L. (1986). Decreased apolipoprotein A-I and B content in plasma of individuals with sickle cell anemia. *Clinical Chemistry, 32*, 226–227.
29. Ginsberg, H. N., Le, N. A., & Gilbert, H. S. (1986). Altered high density lipoprotein metabolism in patients with myeloproliferative disorders and hypocholesterolemia. *Metabolism, 35*, 878–882.

Development ePress online publication date 27 October 2010

Development 137, 3941-3952 (2010) doi:10.1242/dev.051359

Regulation of hematopoietic cell clusters in the placental niche through SCF/Kit signaling in embryonic mouse

Tatsuya Sasaki[1,*,†], Chiyo Mizuochi[1,†], Yuka Horio[1], Kazuki Nakao[2], Koichi Akashi[3] and Daisuke Sugiyama[1]

SUMMARY

Hematopoietic stem cells (HSCs) emerge from and expand in the mouse placenta at mid-gestation. To determine their compartment of origin and define extrinsic signals governing their commitment to this lineage, we identified hematopoietic cell (HC) clusters in mouse placenta, defined as cells expressing the embryonic HSC markers CD31, CD34 and Kit, by immunohistochemistry. HC clusters were first observed in the placenta at 9.5 days post coitum (dpc). To determine their origin, we tagged the allantoic region with CM-DiI at 8.25 dpc, prior to placenta formation, and cultured embryos in a whole embryo culture (WEC) system. CM-DiI-positive HC clusters were observed 42 hours later. To determine how clusters are extrinsically regulated, we isolated niche cells using laser capture micro-dissection and assayed them for expression of genes encoding hematopoietic cytokines. Among a panel of candidates assayed, only stem cell factor (SCF) was expressed in niche cells. To define niche cells, endothelial and mesenchymal cells were sorted by flow cytometry from dissociated placenta and hematopoietic cytokine gene expression was investigated. The endothelial cell compartment predominantly expressed SCF mRNA and protein. To determine whether SCF/Kit signaling regulates placental HC cluster proliferation, we injected anti-Kit neutralizing antibody into 10.25 dpc embryos and assayed cultured embryos for expression of hematopoietic transcription factors. *Runx1*, *Myb* and *Gata2* were downregulated in the placental HC cluster fraction relative to controls. These observations demonstrate that placental HC clusters originate from the allantois and are regulated by endothelial niche cells through SCF/Kit signaling.

KEY WORDS: Hematopoiesis, Hematopoietic stem cells, Niche, Placenta, SCF/Kit, Mouse

INTRODUCTION

During mouse embryogenesis, hematopoiesis begins in the yolk sac (YS), producing mainly primitive erythroid cells at 7.5 days post coitum (dpc). Shortly thereafter, definitive myelo-erythroid progenitor cells appear in the YS, which seed the fetal liver (Cumano et al., 1996; Ferkowicz and Yoder, 2005; Li et al., 2003; McGrath and Palis, 2005; Palis et al., 1999). This process, termed primitive hematopoiesis, diminishes at 12.5 dpc, when definitive hematopoiesis, which sustains the adult blood system through hematopoietic stem cells (HSCs), begins in fetal liver (Sugiyama and Tsuji, 2006). Although there is controversy over where HSCs are generated – in the extra-embryonic YS or intra-embryonic para-aortic-splanchnopleural mesoderm (P-Sp)/aorta-gonad-mesonephros (AGM) region – recent studies suggest that both the YS and P-Sp/AGM region contain HSCs capable of reconstituting adult bone marrow hematopoiesis (Cumano et al., 1996; Matsuoka et al., 2001; Medvinsky and Dzierzak, 1996; Samokhvalov et al., 2007; Yoder et al., 1997a; Yoder et al., 1997b). Thereafter, these AGM HSCs are thought to circulate and colonize fetal liver, where HSC expansion occurs (Cudennec et al., 1981; Ema and Nakauchi, 2000; Houssaint, 1981; Johnson and Moore, 1975; Sugiyama et al., 2005). In addition to these sites, several reports suggest that the placenta functions not only in gas exchange and fetal nutrition but also in hematopoiesis at approximately mid-gestation (Dancis et al., 1968; Dancis et al., 1977; Melchers, 1979). It is also reported that a significant proportion of hematopoietic progenitor cells (HPCs), including highly proliferative potential colony forming cells (HPP-CFCs), are located in the mouse placenta (Alvarez-Silva et al., 2003). HSCs are detected at this site by 11.5 dpc and the number of long-term reconstituting (LTR)-HSCs dramatically increases from 11.5 dpc to 12.5 dpc, resulting in a 15-fold increase in HSC activity compared with that of the AGM region (Gekas et al., 2005; Ottersbach and Dzierzak, 2005). Taken together, these findings indicate that mouse placenta is likely to be a site for HSC generation and expansion at mid-gestation.

HSCs are regulated by intrinsic programming and by extrinsic signaling from so-called niche cells. However, it is unclear how HSC generation and expansion is regulated in the placenta. To address this issue, we identified hematopoietic cell (HC) clusters, defined as cells expressing embryonic HSC markers such as CD31 (Pecam1 – Mouse Genome Informatics), CD34 and Kit, by immunohistochemistry, enabling us to follow the origin of HC clusters and identify surrounding niche cells. We then used vital dye labeling to demonstrate that HC clusters in placenta originate from the allantois, an embryonic compartment of the placenta. Furthermore, we showed that HC clusters are regulated by vascular niche cells through SCF (Kitl – Mouse Genome Informatics)/Kit signaling.

MATERIALS AND METHODS

Immunohistochemistry

Mouse embryos were dissected out and fixed in 2% paraformaldehyde in PBS, followed by equilibration in 30% sucrose in PBS. Placentas were embedded in OCT compound (SAKURA, Tokyo, Japan) and frozen in liquid nitrogen. Tissues were sliced at 20 μm with a Leica CM1900 UV cryostat, transferred to glass slides (Matsunami, Osaka, Japan) and dried thoroughly. Sections were blocked in 1% BSA in PBS and incubated in

[1]Department of Hematopoietic Stem Cells, SSP Stem Cell Unit, Kyushu University Faculty of Medical Sciences, Fukuoka 812-8582, Japan. [2]Laboratory for Animal Resources and Genetic Engineering Animal Resource Unit, Center for Developmental Biology, RIKEN, Kobe 650-0047, Japan. [3]Department of Medicine and Biosystemic Science, Kyushu University Graduate School of Medical Sciences, Kyushu University, Fukuoka 812-8582, Japan.

*Author for correspondence (ds-mons@yb3.so-net.ne.jp)
†These authors contributed equally to this work

Accepted 21 September 2010

PBS containing 1% BSA with appropriate dilutions of the following primary antibodies: goat anti mouse Kit (1:500; R&D Systems, Minneapolis, MN), rat anti mouse-CD31 (1:500; BD Biosciences, San Diego, CA), rat anti mouse-CD34 (1:500; BD Biosciences), rat anti-mouse CD41 (1:300; BioLegend, San Diego, CA), rat anti-mouse CD45 (1:300; BioLegend) and rat anti-mouse F4/80 (1:300; BioLegend) at 4°C overnight. After washing in PBS three times, sections were incubated with appropriate dilutions of the following secondary antibodies: Alexa Fluor 488 donkey anti-rat IgG (1:300; Invitrogen, Carlsbad, CA) and Alexa Fluor 568 donkey anti-goat IgG (1:300; Invitrogen), as well as TOTO-3 (1:1500; Invitrogen) to stain nuclei, at room temperature for 30 minutes. Samples were mounted on coverslips using fluorescent mounting medium (Dako Corporation, Carpinteria, CA) and were assessed using a FluoView 1000 confocal microscope (Olympus, Tokyo, Japan). Cell aggregates consisting of more than four Kit/CD31 or Kit/CD34 double-positive cells were defined as a hematopoietic cluster.

Cell preparation

Placentas without deciduas and umbilical vessels were used to obtain a single cell suspension. Tissues were passed through 21-gauge needles, incubated with 1 mg/ml collagenase in medium supplemented with 10% fetal bovine serum for 30 minutes at 37°C and filtered through 40 μm nylon cell strainers (BD Biosciences). In analysis and sorting of HSCs, density gradient centrifugation using lymphocyte cell separation medium (Cedarlane Laboratories, Eugene, OR) was performed to harvest mononuclear cells. After centrifugation, the cell pellet was used as the placental cell population.

Flow cytometry and cell sorting

As macrophages are found in HSC preparations (CD31, CD34, Kit), anti-mouse F4/80 antibody was added to identify and to exclude them from analysis. Antibodies used for analysis of the HSC population were: FITC-conjugated anti-mouse CD41 (eBioscience, San Diego, CA), FITC-conjugated anti-mouse Sca-1 (eBioscience), FITC-conjugated anti-mouse EPCR (endothelial protein C receptor) (known as CD201) (Stem Cell Technologies, Vancouver, BC), PE-conjugated anti-mouse CD31 (BD Biosciences), APC-conjugated anti-mouse F4/80 (BioLegend), PE-Cy7-cojugated anti-mouse CD45 (BioLegend), APC-Cy7-conjugated anti-mouse Kit (eBioscience) and Pacific Blue-conjugated anti-mouse CD34 (eBioscience). For endothelial and mesenchymal cell populations, FITC-conjugated anti-mouse Ter-119 (eBioscience), PE-conjugated anti-mouse CD31 (BD Biosciences), APC-conjugated anti-mouse Kit (BD Biosciences), PE-Cy7-cojugated anti-mouse CD45 (BioLegend) and Pacific Blue-conjugated anti-mouse CD34 (eBioscience) were used. Flow cytometric analysis and cell sorting were carried out using a FACS Aria cell sorter (BDIS, San Jose, CA). The data files were analyzed using FlowJo software (Tree Star, San Carlos, CA).

RNA extraction and real-time PCR analysis

Total RNA was isolated using the RNAqueous 4PCR kit (Ambion, Austin, TX). mRNA was reverse transcribed using a High-Capacity RNA-to-cDNA kit (Life Technologies, Carlsbad, CA). The quality of cDNA synthesis was evaluated by amplifying mouse β-actin using PCR. Thirty thermal cycles were used as follows: denaturation at 95°C for 10 seconds, annealing at 60°C for 20 seconds, followed by extension at 72°C for 20 seconds. Gene expression levels were measured by real time-PCR with TaqMan Gene Expression Master Mix and StepOnePlus real-time PCR (Life Technologies). All probes were from TaqMan Gene Expression Assays (Life Technologies). All analyses were performed in triplicate wells; mRNA levels were normalized to β-actin and the relative quantity (RQ) of expression was compared with a reference sample.

Enzyme-linked immunosorbent assay

Proteins were extracted from a flow-sorted endothelial and mesenchymal cell population using a Q Proteome Mammalian Protein Preparation kit (Qiagen, Valencia, CA). SCF in both populations was assayed using an (enzyme-linked immunosorbent assay) ELISA kit (Mouse SCF Immunoassay, R&D Systems), according to the manufacturer's instructions. The optical density was measured in a Thermo Multiskan EX plate reader (Thermo Fisher Scientific, Waltham, MA).

Laser capture micro-dissection

For this procedure, embryos were not fixed and equilibration in sucrose in PBS was not undertaken. Tissues sliced at 20 μm on a cryostat were transferred to glass slides (Matsunami), placed on ice and immediately stored at –80°C until use. After thawing, frozen cryosections were washed in PBS three times and incubated with 1:500 goat anti Kit (R&D Systems) for 60 minutes. After washing in PBS three times, sections were incubated with 1:300 Alexa Fluor 488-conjugated donkey anti-goat IgG (Invitrogen) for 60 minutes to detect Kit-positive cells. In this analysis, fluorescent Kit-positive cell aggregates were considered to be HC clusters, and surrounding cells were marked and cut by laser. Those cells were captured as niche cells and transferred to microcentrifuge tubes containing 10 μl extraction buffer using a Pico Pure RNA Isolation Kit (Molecular Devices, Silicon Valley, CA). Laser capture micro-dissection (LCM) was carried out using an ArcturusXT Laser Capture Microdissection System (Molecular Devices). Immunohistochemistry for LCM was carried out at 4°C, and all solutions were treated with diethylpyrocarbonate (Wako, Osaka, Japan).

CM-DiI labeling of the allantois

CM-DiI (Invitrogen), which binds to the cellular membrane, is non-toxic and remains fluorescent for at least for 4 days, was injected into the basal part of allantois of ICR mouse embryos at 8.25 dpc, prior to chorio-allantoic fusion (Downs and Harmann, 1997). Injected embryos were subjected to whole embryo culture (WEC). Dissection and manipulation of embryos was completed within an hour of starting WEC (Sugiyama et al., 2007).

Intra-cardiac injection

For this procedure, 0.2-0.5 μl of anti-Kit neutralizing antibody (ACK2) (eBioscience) and purified rat IgG2b (isotype control; eBioscience) were administered to ICR mouse embryos at 10.25 dpc, a stage at which we can cut the avascular area of yolk sac with minimal bleeding and inject materials into the heart, by intra-cardiac injection, as previously described (Kulkeaw et al., 2009; Sugiyama et al., 2003). Briefly, embryos in PBS were visualized under a stereomicroscope (Leica Microsystems MZ6, Wetzlar, Germany). Both uterus and deciduo capsularis were removed, and the yolk sac was cut along the yolk sac arteries with care to avoid excessive hemorrhage. The amnion was opened to allow needle access to the heart. The needle was made from glass capillary tubes (Narishige GC-10, Japan) using a micropipette puller (Narishige, Tokyo, Japan). Injected embryos were placed in the WEC system within 1 hour of isolation.

Whole mouse embryo culture (WEC)

Injected embryos were transferred to culture bottles containing rat serum supplemented with 2 mg/ml glucose in a WEC system (Ikemoto Scientific Technology, Tokyo, Japan) and cultured for 6 hours in the case of intra-cardiac injection or 42 hours in the case of CM-DiI labeling at 37°C in the dark with a continuous supply of gas (60% O_2 and 5% CO_2 balanced with N_2) (Kulkeaw et al., 2009; Osumi-Yamashita et al., 1997; Sugiyama et al., 2003; Sugiyama et al., 2005; Sugiyama et al., 2007). After WEC, embryos exhibiting no conspicuous bleeding or anomalies were analyzed.

Mutant strains

Runx1$^{+/-}$ mouse strains were kindly provided by Dr N. Speck. *Evi1*$^{-/-}$ and *Myb*$^{-/-}$ mouse strains were obtained from the Jackson Laboratory (Bar Harbor, ME, USA).

RESULTS

Visualization and characterization of HC clusters in the mouse placenta

Previous studies have identified placental HC clusters primarily by microscopic inspection (Ottersbach and Dzierzak, 2005; Rhodes et al., 2008). To extend these studies, quantify clusters, understand their relationship with other placental components and identify